

Supporting Information

© Wiley-VCH 2011

69451 Weinheim, Germany

**Interfacial Photoreduction of Supercritical CO₂ by an
Aqueous Catalyst****

*Manuel A. Méndez, Patrick Voyame, and Hubert H. Girault**

anie_201100828_sm_miscellaneous_information.pdf

Supporting Information

1. Electrochemical Characterization of $[\text{Ni(II)Cyclam}]\text{Cl}_2$

In first place, electrochemical characterization of the catalyst was carried out. With this purpose, cyclic voltammograms were obtained in absence and presence of CO_2 . The working electrode was a glassy carbon disk (area = 0.13 cm^2), polished using 1 and $0.05 \mu\text{m}$ alumina and sonicated in deionized water prior to use. As it can be seen in Fig. S1, a marked increase in the cathodic current alongside the shift of this signal towards less negative values is observed in presence of CO_2 for the signal corresponding to $\text{Ni(II)L}^{2+}/\text{Ni(I)L}^+$. This behavior is in accordance with an electrocatalytic reductive process.

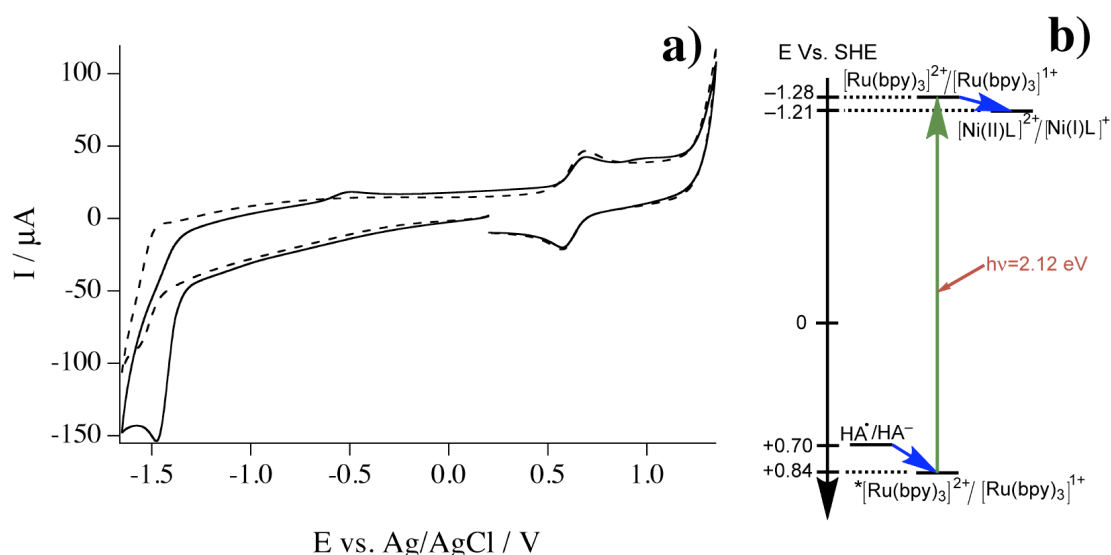


Fig. S1. a) Cyclic voltammogram of a solution of $[\text{Ni(II)cyclam}]\text{Cl}_2$ 2 mM in KCl 0.1 M in absence (dashed line) and in presence of CO_2 (solid line) over a glassy carbon electrode. Scan rate = 100 mV s^{-1} . CE = Pt, RE = Ag/AgCl (KCl 3M). b) Energy diagram illustrating the photosensitized reduction of Ni(II)cyclam .

2. Spectrophotometric determination of the aqueous pH

As it has been previously reported, the aqueous pH is markedly affected by the presence of CO_2 . Therefore, determination of this value as a function of the CO_2 pressure in the reactor was carried out. For that purpose, absorbance measurements of various pH indicators were driven using a three sapphire window cell with an optical path length of 10 cm.

Thus, bromophenol blue was employed in the case where the aqueous phase did not contain any buffer, as it can be observed in Fig.S2. It is then confirmed a dramatic decrease in the pH, as previously reported.^[1]

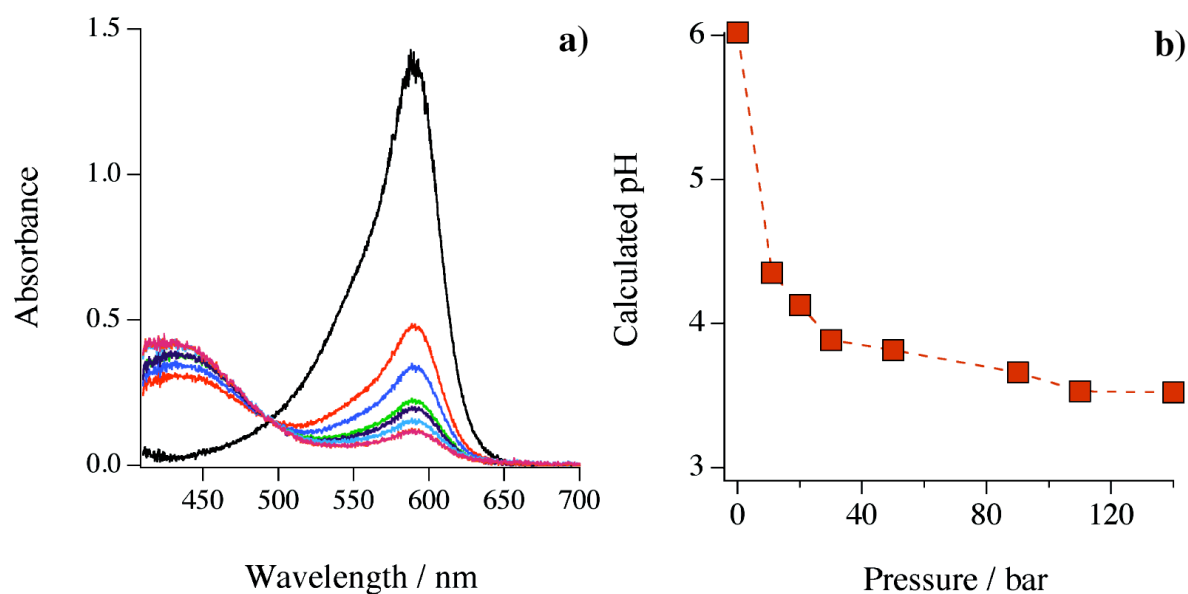


Fig. S2. (a) Visible spectra of an aqueous solution of bromophenol blue 2×10^{-5} M at pressures of 1, 11, 20, 30, 50, 90, 110 and 140 bar. (b) pH as a function of pressure.

Nonetheless, in presence of sodium ascorbate 0.5 M, the latter plays a buffering role keeping always the pH slightly above 5, as it can be deduced from the absorbance values presented in Fig. S3. In this case, bromocresol purple was employed as pH indicator instead of bromophenol blue.

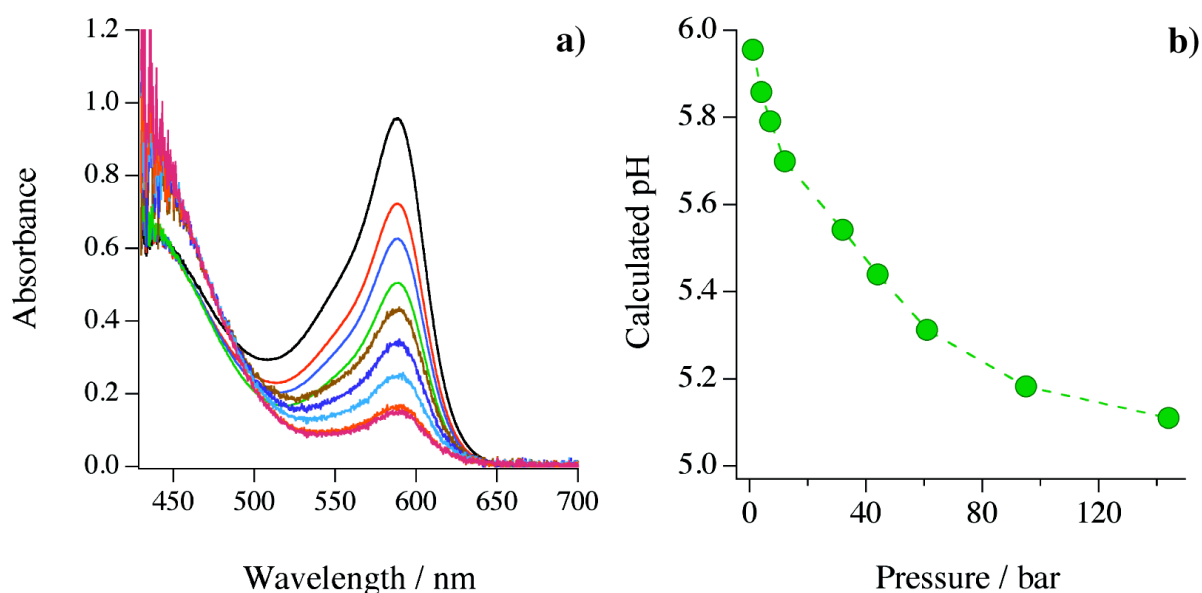


Fig. S3. (a) Visible spectra of an aqueous solution of bromocresol purple 2×10^{-5} M at pressures of 1, 4, 7, 12, 32, 44, 61, 95 and 144 bar. (b) pH as a function of pressure.

3. Gas chromatography

As mentioned in the experimental section, a gas chromatograph was employed to determine the amount of CO present in the samples upon decompression of the reactor. In a typical experiment, two autoclaves of 40 mL capacity each were connected in series to the reactor. The first one is utilized as a liquid trap whereas the second is employed as the collection vessel from which the sample is finally injected into the GC. Gas samples were obtained after slow decompression down to pressures in the interval between 50 to 60 bar. Injection to the GC was carried out using an injection port connected to a six-way valve, where a 1 mL loop was filled with the sample and finally injected into the column. At the same time, post-column conversion to CH₄ was carried out in a methanizer operated at 400 °C and finally detected by a flame ionization detector. Prior to any sample analysis, a CO standard of a known concentration (commonly 500 ppm) was injected. Fig. S4 illustrates chromatograms obtained for the CO standard and the gas sample obtained for exp. 3.

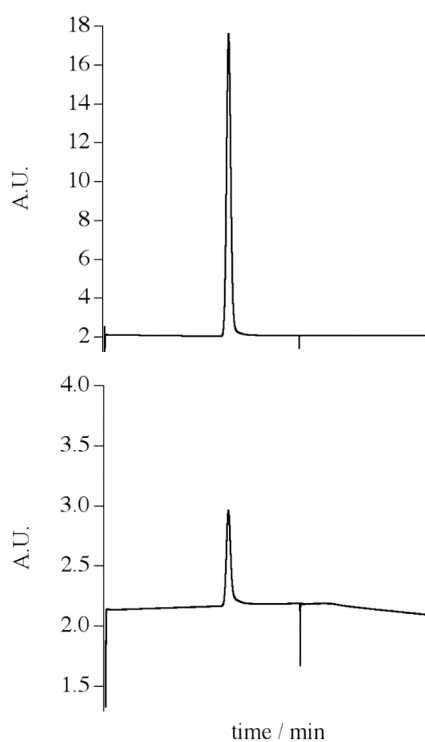


Fig. S4. Gas chromatographs of a 500 ppm CO standard in N₂ (upper figure) and a sample collected after decompression for the exp. 3 (lower figure).

4. Ion transfer voltammetry

In order to prove the relative lipophilic character of the catalyst, ion transfer voltammograms were conducted at the water/1,2-dichloroethane (DCE) interface. The cell employed for these experiments is as follows:

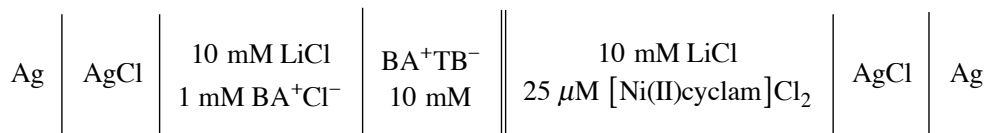


Fig. S5 presents the cyclic voltammograms obtained for Ni(II)cyclam. In this figure, a reversible ion-transfer wave at *ca.* 0.27 V can be clearly recognized. From this potential value, a free Gibbs energy of transfer from DCE to water ($\Delta G_{tr,o \rightarrow w}^{\ominus, \text{Ni(II)L}^{2+}}$) of -52 kJ mol^{-1} can be estimated. Variation of the scan rate also reveals that this is a diffusion-controlled process. Furthermore, the peak separation extrapolated to zero scan rate corresponds to 35 mV, which is very close to the 30 mV value expected for the reversible transfer of a doubly charged ion.

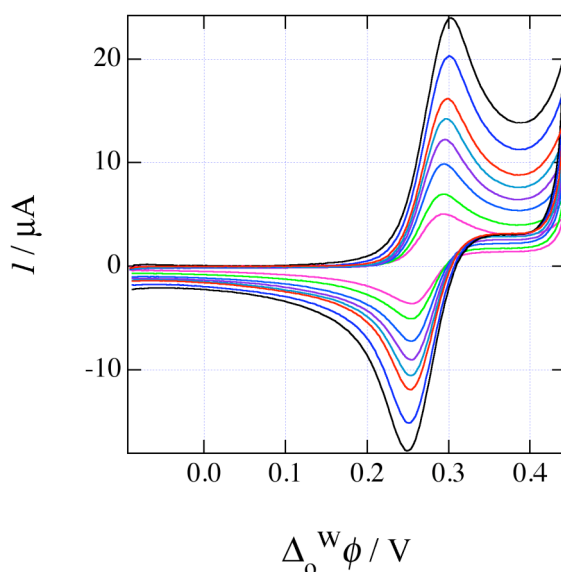


Fig. S5. Ion transfer voltammograms at the interface formed between an aqueous solution of LiCl 10 mM and [Ni(II)cyclam]Cl₂ 25 μM and BATB 10 mM in 1,2-dichloroethane. Scan rates = 5, 10, 20, 30, 40, 50, 75 and 100 mV s⁻¹.

5. Interfacial tension measurements at the water–air interface

In first place, surface tension measurements at the air–water interface were carried out with a Wilhelmy plate (Nima Technologies, Model 6502). Interfacial tension measurements as a function of the concentration of Ni(II)Cyclam were treated according to the Gibbs adsorption equation:

$$\Gamma_{\text{NiCyc}} = - \left(\frac{d\gamma}{d\mu_{\text{NiCyc}}} \right)_{T,p,\mu_i} = - \frac{1}{RT} \left(\frac{d\gamma}{d \ln a_{\text{NiCyc}}} \right)_{T,p,\mu_i} \approx - \frac{1}{RT} \left(\frac{d\gamma}{d \ln C_{\text{NiCyc}}} \right)_{T,p,\mu_i} \quad (\text{SI.1})$$

Surface coverage values were fitted to a Langmuir isotherm. The values obtained for the free Gibbs energy of adsorption (ΔG_{ads}^{\ominus}) and the maximum surface coverage (Γ_{max}) are -10 kJ mol^{-1} and $1.09 \mu\text{mol m}^{-2}$, respectively.

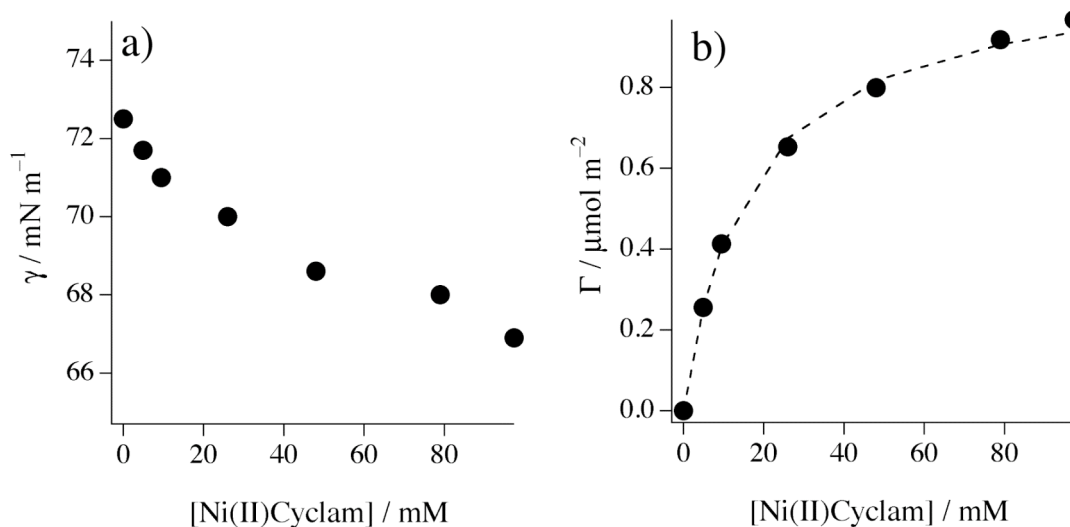


Fig. S6. (a) Air–water interfacial tension as a function of the Ni(II)Cyclam aqueous concentration. (b) Surface excess concentrations calculated from the Gibbs adsorption equation (solid circles). Fitting to a Langmuir isotherm is presented in dashed lines.

The maximum surface coverage can be analogously expressed as the area occupied per molecule at the interface, yielding a valued of 152 \AA^2 per molecule of complex adsorbed. The latter indicates that complex molecules adsorbed at the water–air interface could adopt a planar orientation.

6. Pendant drop analysis of the water–scCO₂ interface

As adsorption of Ni(II)Cyclam occurs at the water–air interface, this is also very likely to occur at the water–scCO₂ interface. In order to prove this hypothesis a custom–built pendant drop setup was employed with which aqueous droplets of $15 \mu\text{L}$ were formed at the tip of a stainless steel needle (inner diameter = 0.5 mm). Images of the drop were recorded with a high-resolution handheld microscope (Proscope HR, Bodelyn Technologies) mounted in front of the view-cell. Potentially destabilizing pressure gradients were successfully avoided by operating the CO₂ piston pump at a constant pressure of 140 bar , while the pump dedicated to the injection of water was operated at a constant flow rate of $10 \mu\text{L min}^{-1}$. Thus, after an injection period of 90 seconds stable and reproducible pendant drops of $15 \mu\text{L}$ were obtained. Image acquisition was always performed after an equilibration period of 10 seconds and further analysis was carried out with Mathematica 8.0 (Wolfram research). Drop profiles can be obtained by

applying a Shen–Castan algorithm to the raw image. All measurements were done by triplicate. An illustration of the droplets obtained is illustrated in Fig. S7 from which it can be observed a slight elongation of the droplet in presence of Ni(II)-Cyclam 50 mM (Fig. S6b), which is equally observed once the profile of the droplet is extracted (Fig. S6c and S6d). From these, and using the selected plane method for determining the interfacial tension previously described by Andreas *et al.*,^[2] the parameter S was determined and is equal to:

$$S = \frac{d_S}{d_E} \quad (\text{SI.2})$$

being d_E the diameter at the equator and d_S the diameter of the droplet determined in a parallel plane located at a distance d_E from the apex defined as the point where the axis of rotation cuts the drop. Thus, in absence of Ni(II)Cyclam an average value of S of 0.517 is obtained while in its absence is 0.537.

According to the theory, the shape of a static pendant drop can be described by the Laplace equation:

$$\frac{d\theta}{dS} = 2 - \beta Y - \frac{\sin(\theta)}{X} \quad (\text{SI.3})$$

Eq.(SI.3) can be numerically solved by combining it with the following two additional equations:

$$\frac{dX}{dS} = \cos(\theta) \quad (\text{SI.4})$$

$$\frac{dY}{dS} = \sin(\theta) \quad (\text{SI.5})$$

where S the normalized radius of curvature (s/b), $X = x/b$, $Y = y/b$ and the normalization constant, b , is the curvature at the apex of the drop.

The parameter β is given by:

$$\beta = \frac{\Delta\rho g b^2}{\gamma} \quad (\text{SI.6})$$

γ is the interfacial tension, g the gravitational constant, $\Delta\rho$ the effective density of the drop, *i.e.* the density difference between water and supercritical CO₂ in this particular case. Herein the polynomial approximation proposed by Girault *et al.*^[3] is used in order to determine the parameter β .

$$\beta = 0.02664 + 0.62945S^2 \quad (\text{SI.7})$$

By applying Eq.(SI.7) to the values of S previously found for the two cases, β is estimated to be equal to 0.195 in the absence and 0.208 in the presence of Ni(II)Cyclam. The theoretical profiles presented in Fig.S7e were determined taking into account the values for β aforementioned. Comparable elongation of the droplet is qualitatively observed in the theoretical and experimental drop profiles.

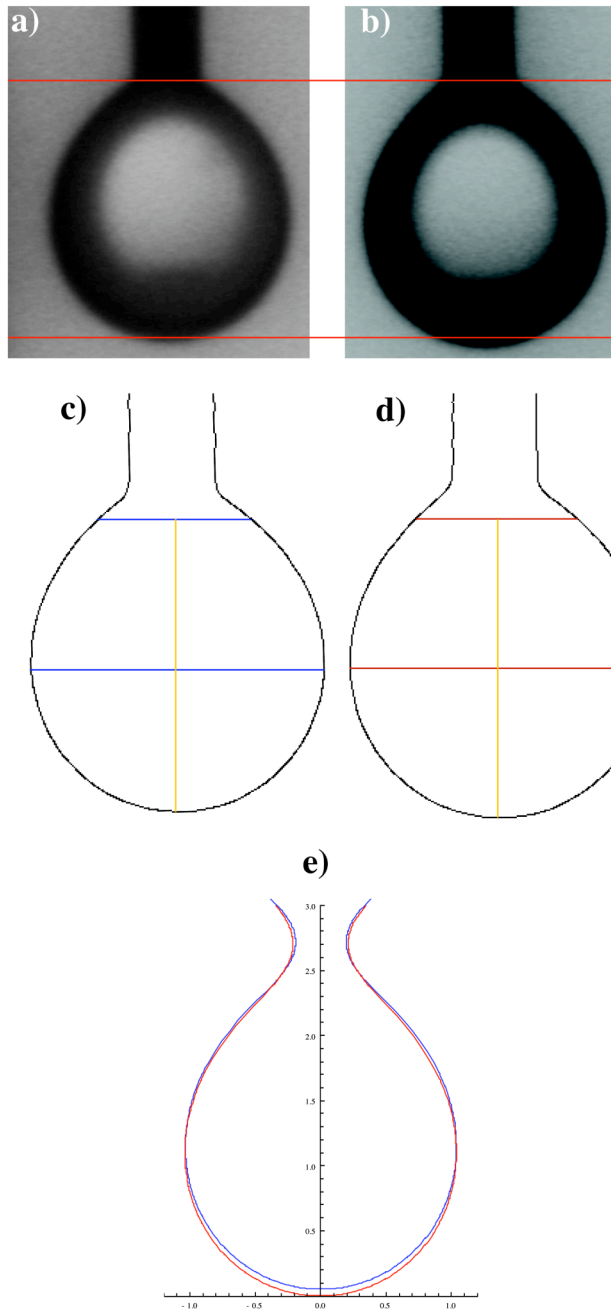


Fig. S7. Images of an aqueous droplet in absence (a) and in presence (b) of Ni(II)Cyclam at a concentration of 50 mM. Profiles extracted using Mathematica after applying a Shen–Castan algorithm are presented in (c) and (d), respectively. For comparison, theoretical profiles calculated (e) from the parameter S obtained for (c) is presented in blue and for (d) in red.

Additionally, if one assumes curvature radius at the apex, b , remains approximately constant for both cases, then:

$$\frac{\beta_{\text{H}_2\text{O}}}{\beta_{\text{NiCyc}}} \approx \frac{\gamma_{\text{NiCyc}}}{\gamma_{\text{H}_2\text{O}}} = 1.067 \quad (\text{SI.8})$$

meaning that according to Eq.(SI.8) the water–supercritical CO_2 interfacial tension diminishes by approximately 6.7% when Ni(II)Cyclam is present.

- [1] C. Roosen, M. Ansorge-Schumacher, T. Mang, W. Leitner, L. Greiner, *Green Chem.* **2007**, 9, 455-458.
- [2] J. M. Andreas, E. A. Hauser, W. B. Tucker, *J. Phys. Chem.* **1938**, 42, 1001-1019.
- [3] H. H. Girault, D. J. Schiffrin, B. D. V. Smith, *J. Electroanal. Chem.* **1982**, 137, 207-217.